LINEAR INDUCTION ACCELERATOR PARAMETER OPTIONS

D. L. Birx, G. J. Caporaso and L. L. Reginato

Lawrence Livermore National Laboratory
University of California
Livermore, CA 94550

UCID--20786

DE86 015003

April 21, 1986

INTRODUCTION

The principal undertaking of the Beam Research Program over the past decade has been the investigation of propagating intense self-focused beams. Recently, the major activity of the program has shifted toward the investigation of converting high quality electron beams directly to laser radiation. During the early years of the program, accelerator development was directed toward the generation of very high current (> 10 kA), high energy beams (> 50 MeV). In its new mission, the program has shifted the emphasis toward the production of lower current beams (< 3 kA) with high brightness (> 10^6 A/(rad-cm)^2) at very high average power levels. In efforts to produce these intense beams, the state of the art of linear induction accelerators (LIA) has been advanced to the point of satisfying not only the current requirements but also future national needs.

Work performed jointly under the auspices of the U.S. Department of Energy by the Lawrence Livermore National Laboratory under contract No. W-7405-ENG-48 and for the Department of Defense under DARPA, ARPA Order No. 4395 and 5316, monitored by Naval Surface Weapons Center under document number N60921-85-PDW0001; SDIO/BMD-ATC MIPR #W31-RPD-53-A127; and SDIO/NSWC reference number B00014-85-WR35514.

ACCELERATOR COMPARISON

Considering the international family of linear accelerators, the LIAs have relatively low gradient but very high current capability. The two-mile Stanford Linear Accelerator (SLAC) consists of a waveguide system that transfers microwave (2856 MHz) power from klystrons to the disk-loaded accelerator structure. This structure is a high-Q (high impedance) cavity that accelerates micropulses (ps) of very low current (amperes) at very high gradients. In contrast, the LIA[1] consists of a simple nonresonant structure where the drive voltage is applied to an axially symmetric gap that encloses a toroidal ferrimagnetic material. The change in flux in this magnetic core induces an axial electric field that provides acceleration for the electrons. This simple nonresonant (low Q) structure acts as a single-turn transformer that can accelerate from hundreds of amperes to tens of kiloamperes, basically limited by the drive impedance. In principle, such a structure can also provide acceleration fields of varying time duration from tens to hundreds of nanoseconds at virtually any repetition rate. The fundamental limits on the operating parameter space are dictated by the requirements of "high current" beam transport physics. Much like SLAC, these limits dictate maximum currents, cell shapes and sizes, so that electron beam motion through the cells does not lead to instabilities and beam breakup (BBU). Other limits on the accelerator pulse format, such as pulse duration and repetition rates, are dictated by limits of the drive system, cells, and switch recovery times. Free-electron laser (FEL) physics requirements for a monoenergetic beam (within 0.5%) during the duration of the pulse imposes further restrictions on the physical dimensions of the accelerator cell.

BEAM D/NAMICS AND CELL DESIGN

Experimental observations on existing accelerators have established a high confidence factor on the theoretical formulation of beam instabilities associated with electron motion through the accelerator structure.[2] For continuity those effects are qualitatively described here.

Resonances in the accelerator cell are excited by the rising current at the head of the beam pulse, and cavity oscillations occur. These oscillations can cause variations in the beam energy that can lead to difficulties in beam transport and a not entirely useful beam for FEL experiments. In addition, the oscillations could cause transverse beam modulation leading to exponential growth down the accelerator and the beam hitting the pipe. The beam interaction with the accelerator cell is minimized by reducing the beam coupling to the cell and by lowering the cell response, or Q. The accelerating gap width is established by choosing a voltage holding safety factor of two or more above the operating voltage. In our case, the spacing chosen is 1/4 inch for 150 kV. The insulator angle was chosen so that all TM modes excited will pass through the ceramic into the ferrite to be absorbed or damped by the ferrite cores. The ceramic is shielded from the electron beam by making the gap slightly re-entrant.

For the 300-MeV accelerator, the electron beam will traverse 2000 gaps. It is expected that the transport will be entirely magnetic with laser guiding as the fall-back position. The mathematical model of the beam-to-cell interaction accurately describes the effect of different parameters. A conservative point design for a BBU gain of 5 and a 3-kA beam sets the pipe diameter at 15 cm. For 500-A beam, the pipe size could be reduced to 4.5 cm diameter.

SCALING OF THE CONCEPTUAL POINT DESIGN

A conceptual point design exists for a 3-kA, 300-MeV accelerator, which has a computed BBU gain on the order of 5. The point design simultaneously satisfies the requirements for high brightness preservation and beam stability against both single particle parametric instabilities and coherent beam-cavity instabilities.

The point design may be scaled if it is desirable to have a different beam current or accelerator length, for example. To avoid parametric instabilities and keep beam envelope flutter to an acceptable level in the quadrupole transport region, we hold the phase advance per focusing period constant; i.e., $k_\beta L$ is held constant where k_β is the betatron wavenumber and L is the period of the quadrupole lattice. For quadrupoles, k_β is proportional to BL/b where B is the pole face field and b is the pipe radius. This proportionality assumes that the ratio of axial length of the quadrupole to L is fixed.

The BBU gain depends on the quantity $\omega_0 Z\ I/k_\beta$ where $\omega_0 Z$ is the coupling impedance of the cavities and I is the beam current. The quantity $\omega_0 Z$ is proportional to w/b^2 where w is the gap width. If we introduce a scaling parameter s to allow for the possibility of different BBU gains, the above relationships become $k_\beta L \propto L^2/b$ = constant, and $\omega_0 Z\ I/k_\beta \propto s$ (we hold the pole face fields of the quadrupoles constant). These may be solved to yield the scaling relations

$$b \propto (wI/s)^{2/3} ,$$

$$L \propto \sqrt{b} \propto (wI/s)^{1/3} ,$$

$$k_\beta \propto L/b \propto 1/\sqrt{b} \propto (wI/s)^{-1/3} .$$

To preserve the scaling of pipe radius in the solenoid section of the accelerator we must also have $B_z \propto (wI/s)^{-1/3}$. Thus, lowering the beam current could allow the use of smaller diameter pipes. This would also require a tighter axial placement of shorter quadrupoles.

In practice, the gap width, w, is made as small as possible consistent with the prevention of arcing across the accelerator gap. The allowed pipe radius versus beam current for different BBU gains can then be determined and is shown in Fig. 1.

HIGH-POWER CELL OPTIMIZATION

We can see that the minimization of BBU growth has established the pipe diameter and gap design. That still leaves the volume of the accelerator core as a free variable determined by the voltage per cell and the effective gradient. The energy loss (W) in the core in one cycle is given by Eq. (1).

$$W = A \cdot z \oint H \cdot dB \qquad (1)$$

where $\oint$ is the area enclosed by the hysterisis loop, A is the cross-sectional area, and z is the axial length, or $A \cdot z$ is the volume (V) of the core. The B-H loop considered is for the appropriate pulse length, which includes all magnetic losses. From Fig. 2 it can be seen that the best choice of materials for short pulse lengths are the nickel-zinc ferrites. Ferrites also have the necessary property of being excellent mode dampening devices. The ferrite cross-sectional area, A, is set by Maxwell's equation

$$V_{acc}\Delta t = A \cdot \Delta B \qquad (2)$$

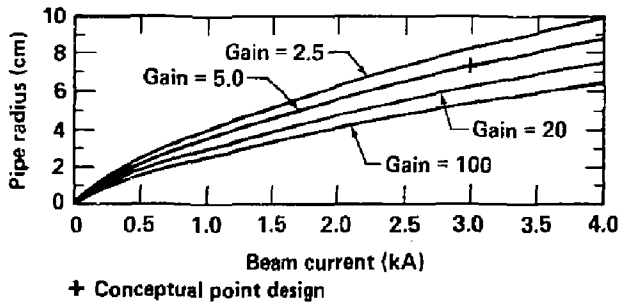

Figure 1. Pipe radius versus beam current for various beam breakup gains scaled from the conceptual point design. In scaling the point design, the phase advance per focusing period has been held constant to preserve brightness and avoid parametric instabilities.

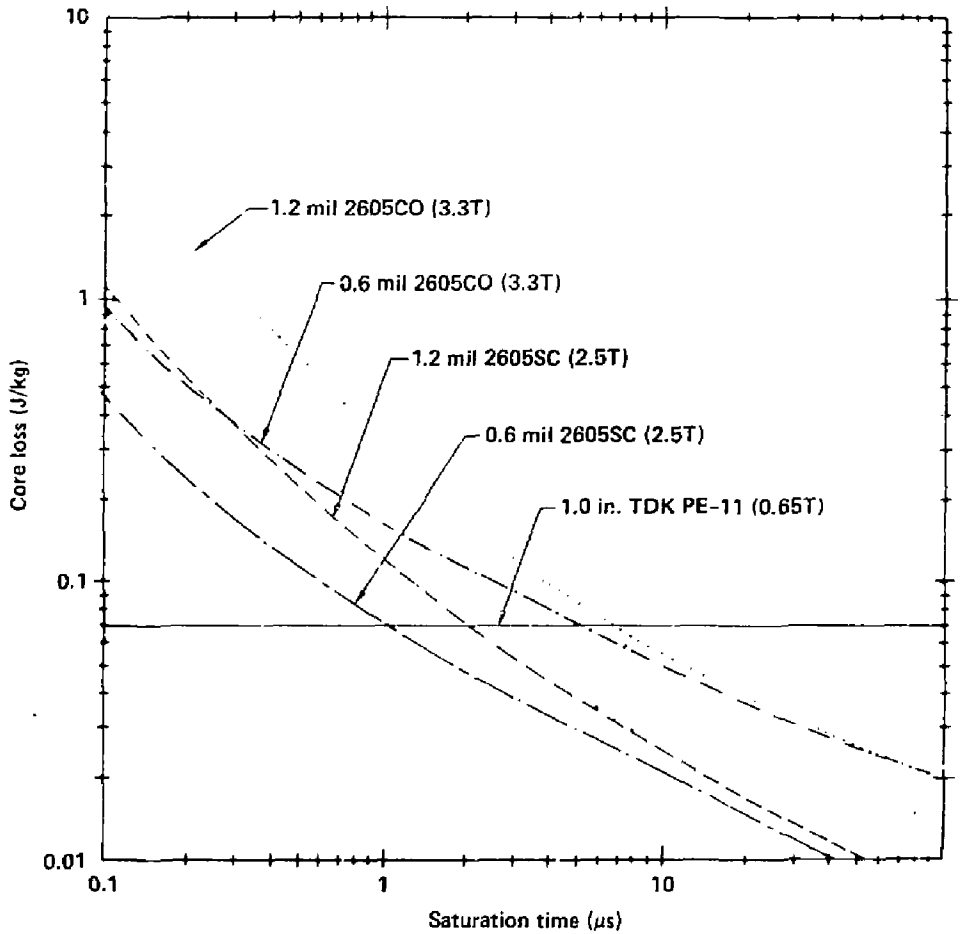

Figure 2. Estimated core losses for different materials.

where V_{acc} is the accelerating potential, Δt is the pulse duration, and ΔB is

the total flux swing.

For the point design V_{acc} = 150 kV, Δt = 75 ns and for ferrites ΔB = 0.6 Wb/cm^2. Then the cross-sectional area A = 187 cm^2. The actual shape of the toroid will be determined by the actual pulse droop and losses that can be tolerated.

The ferrite magnetization current, I_M is given by

$$I_M = \oint H \cdot dl \tag{3}$$

where H is the magnetic intensity, l is the length of path, and I_M is the time-varying current given by

$$I_M = \frac{1}{L} \int_0^t V_{acc} dt \tag{4}$$

where L is the total inductance of the cell given by

$$L = \frac{\mu}{2\pi} \cdot z \ln \frac{r_0}{r_i} \tag{5}$$

where μ is the permeability of the ferrite, z is the axial length, and $r_0(r_i)$ is the outer (inner) radius of the core. Given the best ferrite permeability, the aspect ratio of the ferrite will determine the maximum magnetization or leakage current. Since A is given by Eq. (2), the effective gradient (V_{acc}/z) will determine the volume.

It is important to keep the magnetization losses as a fraction of the total drive not only from an efficiency and heat removal standpoint but also mainly because it becomes increasingly more difficult to compensate for pulse flatness. Figure 3 shows the ferrite core losses for different accelerator designs. The points on the curves reflect the 10-kA design of the Advanced Test Accelerator (ATA), the 3-kA design of the FEL, and a conceptual design of a 500-A accelerator. It can be seen from Eq. (4) and (5) that for lower current LIAs, in order to keep the core losses low, we are directed toward a low-gradient cell. As the peak current level is reduced, BBU scaling also allows a reduction in pipe size (Fig. 1). If we now set the maximum magnetizing (leakage) current in the ferrite at < 20%, the actual cell size (volume) and the gradients will be established.

For the 3-kA point design, from Fig. 3 we can accept a peak magnetization current of 500 A. From Eq. (4) we find that the required $L = 22$ μH at a voltage gradient of 750 kV/m. From Eq. (5) we find that $z \geq 20$ cm. For this design $r_0 \approx 7.5$ cm. The cell design is shown on Fig. 4. The design of an accelerator cell for a 0.5-kA beam would look quite different when the same design criteria is applied. It would be considerably longer (lower gradient).

It has been assumed so far that the accelerator pulse duration was fixed at 75 ns. It is interesting now to scope the effect of varying the pulse duration on the volume of the cell.

The core area, A, is set by Eq. (2) and is given by

$$A = z\,(r_0 - r_i) \quad , \tag{6}$$

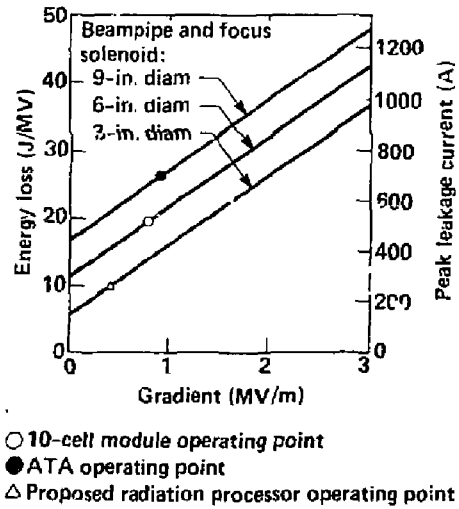

Figure 3 Core losses for TDK ferrite as a function of accelerator gradient at different beampipe diameters. (Linear packing fraction = 0.8; pulse length = 75ns.)

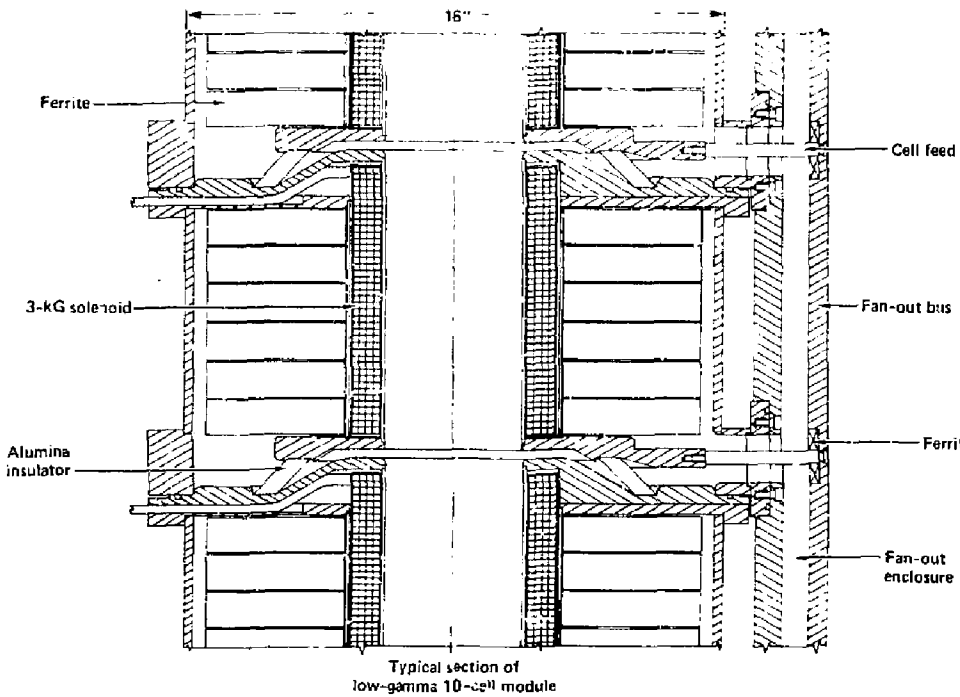

Figure 4. Cross-section of the new 150-kV accelerator cell.

and the volume, V, is given by

$$V = z \cdot \pi (r_0^2 - r_i^2) = \frac{\pi}{z} A^2 \left(\frac{r_0 + r_i}{r_0 - r_i}\right) . \qquad (7)$$

The area of the core varies linearly with pulse length, and the excitation losses vary linearly with the volume. It can be seen in Eq. (7) that accelerator length per MV or inverse gradient has a strong affect on the volume, and hence on cost and weight. At a fixed gradient, r_0 will vary linearly with t, but the volume will vary as r_0^2. The core losses will, therefore, vary as t^2. Figure 5 shows the core loss as a function of different pulse widths. For high-average-power accelerators, the core losses are chosen to be a small fraction of the total energy delivered. Under maximum repetition rate, the inside temperature of the ferrites must be kept below the level where magnetic property degradation occurs.

At a fixed gradient, we pay a severe penalty in energy losses for longer pulse duration. The full-width half-maximum (FWHM) for the FEL accelerator was chosen to be 75 ns at a gradient of 750 kV/m or an energy loss of 18 Joules/MV.

The losses presented by the cell to the driving source vary with time. For the voltage pulse to remain within the energy variations specified by the FEL, a load having a complementary response time must be connected. The output voltage response is given by

$$V_{acc} = V_0 \, e^{-\frac{t}{L/R}} \qquad (8)$$

where L is the cell inductance and R is the driving impedance. The actual compensation could be quite accurate were it not for the nonlinearities in the

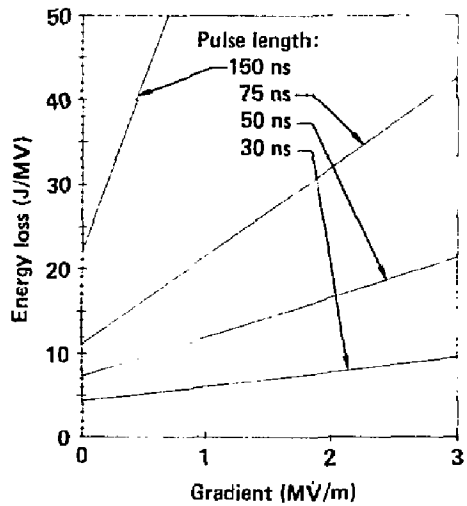

Figure 5. Core loss for TDK ferrites as a function of gradient showing the effect of pulse length on losses. (Beampipe radius = 6-in. diam; linear packing fraction = 0.8.)

changing permeability at different points on the B-H curve. The larger the magnetization losses, the more difficult the compensation becomes. It would not be surprising if several harmonics of compensation were required.

Different limits are imposed on the accelerator cell design. The BBU requirement on the gap and beampipe diameter is a fundamental limit. The beam simply will not be useful if this criteria is not met. The requirements imposed by energy losses are less fundamental and allow some room for design options.

REPETITION RATE LIMITS

The accelerator cell parameters have been determined by requirements imposed by beam dynamics, efficiency, and pulse compensation. No consideration has been given to heat removal from within the ferrite cores. The standard core thickness for LIAs has been one inch. For the point design of the FEL accelerator this corresponds to about 3 J/cell-pulse. The ferrite properties deteriorate with temperature. A rise in temperature ΔT of 30°C above ambient results in an acceptable loss of magnetic flux, ΔB. The maximum average power or repetition rate for different pulse formats can then be calculated. Figure 6 presents the allowable run-time at different repetition rates for a 1-in.-thick ferrite disk.[4] It can be seen that the cell can be operated well beyond any FEL requirements of 5 kHz for 30 sec (* on Fig. 6).

The trend in the design of an FEL accelerator has shifted toward lower currents at the same average power. Since the wavelength of the light amplified sets the total voltage, a lower beam current means either a longer pulse length at the same frequency or the same pulse length at a higher frequency.

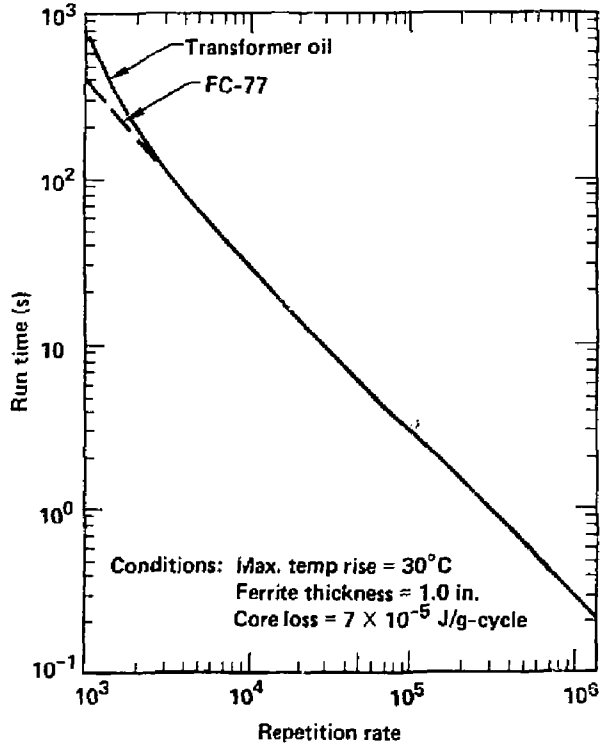

Figure 6. Run-time allowed keeping the ferrite cell temperature rise below 30°C.

A lower energy per pulse would require a redesign of the accelerator cell toward a lower gradient to keep the same overall efficiency. As discussed previously, at a fixed gradient losses vary approximately as t^2. Even at reduced gradient, a wider pulse is unattractive because of the added difficulties in compensation. A lower energy pulse then directs us toward higher repetition rates.

DRIVE SYSTEM LIMITS

The magnetic driver[5] (MAG-I-D) consists of nonlinear inductors that operate from the unsaturated to the fully saturated condition in the pulse compression process.

With the exception of BBU requirements, the same laws that apply to the accelerator cell also apply to the nonlinear magnetics. The device geometry is dictated by the small fraction of energy loss that is allowed within the cores. The limits of this device are plotted on Fig. 7. The operating limits of the magnetic driver are closer to the point design because the material used (Metglas) has higher losses (eddy currents) than ferrites at short saturation times (Fig. 2). Ferrite can and has been used in some of our early pulsers for shorter pulse duration and higher frequencies. The only disadvantage being that a greater volume is required due to its lower flux swing.

The most stringent limitation in terms of repetition rates is the thyratron switch in the intermediate energy storage. After the energy delivery cycle, this device requires 25 to 50 μs for recovery time before voltage can be reapplied. This device does not impose a limit on the power delivered since many can be paralleled. In a multiplexed arrangement where separate

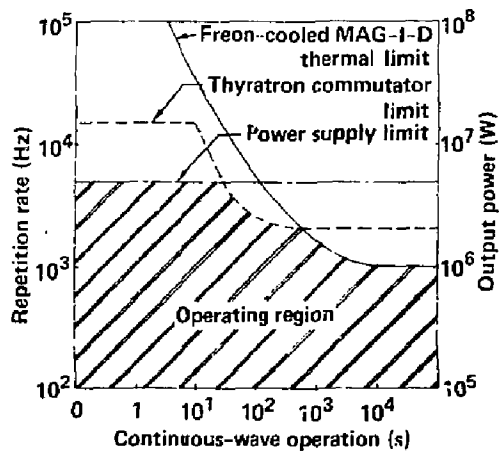

Figure 7. MAG-I-D operating power level for different run times showing both the magnetic cooling limits and thyratron commutation limits.

inter- mediate energy stores are tied to the same MAG-I-D, one could possibly envision a maximum repetition rate of 30 kHz. In a branched magnetics system where the switch is isolated from the backward pulse, the repetition rates can go well beyond the 30 kHz. There are other switches that have faster recovery times, but their power handling capability is many orders of magnitude lower than the thyratron. Perhaps continued development will make them useful for our application at higher repetition rates.

SUMMARY

We have provided quantitative guidelines for the selection of the accelerator point design. Control of beam instabilities dictates the size of the acceleration gap and beam pipe. Compensation for pulse flatness and core losses dictate the effective gradient or aspect ratio of the core. It is clear that it becomes increasingly difficult to design efficient lower current and wider pulse width linear induction accelerators. Those requirements lead to lower gradients and lower efficiencies.

REFERENCES

1. L. L. Reginato et al., "The ATA Accelerator, a 50 MeV, 10 kA Induction Linac," IEEE Transaction on Nuclear Science, Vol. NS-30, No. 4, Aug 1983.

2. R. J. Briggs et al., Theoretical and Experimental Investigation of the Interaction Impedances and Q Values of the Accelerating Cells, Lawrence Livermore National Laboratory, Livermore, Calif., UCRL-92095 (1984).

3. D. L. Birx et al., A Collection of Thoughts on the Optimization of Magnetically Driven Induction Linacs for the Purpose of Radiation Processing, Lawrence Livermore National Laboratory, Livermore, Calif., UCRL-92828 (1985).

4. J. Van Sant, Lawrence Livermore National Laboratory, Livermore, Calif., private communication (1986).

5. D. L. Birx et al., The Applications of Magnetic Switches as Pulse Sources for Induction Linacs, IEEE Transactions on Nuclear Science, Vol. NS-30, No. 4, Aug 1983.

0272a/0005a